gested that the changes in the phosphorescence lifetimes were due to changes in the mixing between the $^3(n\pi^*)$ and $^3(\pi\pi^*)$ states caused by their changing energy differences. A smaller polarizing power (charge/radius ratio) for the metal ion would lead to a smaller energy difference and larger mixing between the $^3(n\pi^*)$ and $^3(\pi\pi^*)$ states, causing the lifetime of the triplet state to shorten because of increased $^3(n\pi^*)$ character. We find no need to involve nor evidence to support this explanation. The changes in the phosphorescence lifetimes can result simply from changes in the spin-orbit mixing between the $^1(n\pi^*)$ and $^3(\pi\pi^*)$ states.

Acknowledgment. We thank M. M. Olmstead for providing analyses of some of the complexes by x-ray diffraction methods.

Registry No. $NH_4(acac)$, 86392-33-8; $Be(acac)_2$, 10210-64-7; $Mg(acac)_2$, 14024-56-7; $Zn(acac)_2$, 14024-63-6; $Ca(acac)_2$, 17372-36-0; $Ba(acac)_2$, 17372-35-9; $Ca(acac)(OAc)\cdot 2H_2O$, 86392-34-9.

Photochemistry of $Ru(bpy)_3^{2+}$. Solvent Effects

Jonathan V. Caspar and Thomas J. Meyer*

Contribution from the Department of Chemistry, University of North Carolina, Chapel Hill, North Carolina 27514. *Received July 23, 1982*

Abstract: The excited-state lifetime of the metal-to-ligand charge-transfer (MLCT) excited state or states of $Ru(bpy)_3^{2+}$ has been measured in a series of solvents at a series of temperatures. The data can be fit to the equation $\tau(T)^{-1} = k + k'^0 \exp[-(\Delta E'/k_B T)]$ where k is the sum of the radiative (k_r) and nonradiative (k_{nr}) rate constants for decay of the MLCT state(s) and the temperature-dependent term involves a thermally activated transition from the MLCT state to a low-lying state or states presumably d-d in character. From a combination of lifetime and emission quantum yield measurements, values for k_r and k_{nr} have been obtained in the series of solvents. From the variations of the various kinetic parameters with solvent the following conclusions can be reached: (1) k_r is only slightly solvent dependent; (2) the variations in k_{nr} and emission energy with solvent are in quantitative agreement with the predictions of the energy gap law for radiationless transitions; and (3) the solvent dependence of the kinetic parameters k'^0 and $\Delta E'$, which characterize the MLCT → dd transition, can be considered in the context of electron-transfer theory including the observation of a linear relationship between ln k'^0 and $\Delta E'$ (Barclay-Butter plot). In a final section the implications of solvent effects on the use of $Ru(bpy)_3^{2+*}$ as a sensitizer are discussed.

We have shown that the energy gap law can be applied to nonradiative decay in a series of polypyridyl complexes of Os(II).[1,2] The studies were based on the metal-to-ligand charge-transfer (MLCT) excited states of the two series of complexes (phen)$Os^{II}L_4^{2+}$ and (bpy)OsL_4^{2+} (bpy is 2,2'-bipyridine, phen is 1,10-phenanthroline; L = $^1/_2$bpy, $^1/_2$phen, pyridine, PR_3, Me_2SO, CH_3CN, ...). The nature of the experiment was to show from excited-state lifetime and emission measurements that plots of ln k_{nr} vs. E_{em} are linear where k_{nr} is the nonradiative decay rate constant and E_{em} the emission energy. In addition, it was possible to account for the origin of the solvent dependence of k_{nr} on the basis of the energy gap law using the series of Os-phen based MLCT excited states.[3] In these studies, radiative rate constants, k_r, for excited-state decay, were shown to be relatively insensitive to variations either in complex or in solvent.

The earlier studies based on the Os(II) complexes are part of a larger effort to explore in detail the photochemical and photophysical properties of MLCT excited states. In many ways the "parent" compound associated with MLCT excited states is $Ru(bpy)_3^{2+}$. The excited-state electronic structures of $Ru(bpy)_3^{2+}$ and related complexes have been investigated by spectroscopic studies,[4] low-temperature emission and lifetime measurements,[5] and theoretical studies.[6] The excited state(s) of $Ru(bpy)_3^{2+}$ has been frequently used in sensitization processes based on electron-transfer quenching.[7]

Because of its importance, it is desirable to establish in detail the photochemical and photophysical properties of $Ru(bpy)_3^{2+}$. Compared to related complexes of Os(II), there is an additional complication for complexes of Ru(II) associated with the intervention of a low-lying d-d state or states. Evidence for the d-d state has come from temperature-dependent lifetime[5b-d] and photochemical ligand loss experiments.[5d,8] In equivalent polypyridyl ligand environments, d-d states do not appear to play an important role for complexes of Os(II) compared to Ru(II). The major factor is no doubt that $10Dq$ is ~30% higher in the third transition series compared to the second[9] so that low-lying d-d states occur at higher energies and are well removed from the emitting MLCT states.

We report here on the results of a solvent-dependence study on the lifetime and emission energies for the excited state(s) of $Ru(bpy)_3^{2+}$, $Ru(bpy)_3^{2+*}$. $Ru(bpy)_3^{2+*}$ has been used as a sensitizer in a variety of media and it is important to establish and to attempt to rationalize the solvent dependence of its excited-state properties. For the case of $Ru(bpy)_3^{2+}$, the problem is complicated by the presence of the low-lying d-d state(s) but, on the other hand, that complication offers an advantage. The advantage is that solvent efects can be explored both as to how they affect

(1) Kober, E. M.; Sullivan, B. P.; Dressick, W. J.; Caspar, J. V.; Meyer, T. J. *J. Am. Chem. Soc.* **1980**, *102*, 1383.
(2) Caspar, J. V.; Kober, E. M.; Sullivan, B. P.; Meyer, T. J. *J. Am. Chem. Soc.* **1982**, *104*, 630.
(3) Caspar, J. V.; Kober, E. M.; Sullivan, B. P.; Meyer, T. J. *Chem. Phys. Lett.* **1982**, *91*, 91.
(4) (a) Felix, F.; Ferguson, J.; Gudel, H. U.; Ludi, A. *J. Am. Chem. Soc.* **1980**, *102*, 4096. (b) Fujita, I.; Kobayashi, H. *Inorg. Chem.* **1973**, *12*, 2758. (c) Palmer, R. A.; Piper, T. S. *Ibid.* **1966**, *5*, 864.
(5) (a) Hager, G. D.; Crosby, G. A. *J. Am. Chem. Soc.* **1975**, *97*, 7031. (b) Allsopp, S. R.; Cox, A.; Kemp, T. J.; Reed, W. J. *J. Chem. Soc., Faraday Trans. 1* **1977**, 1275. (c) Van Houten, J.; Watts, R. J. *J. Am. Chem. Soc.* **1976**, *98*, 4853. (d) Durham, B.; Caspar, J. V.; Nagle, J. K.; Meyer, T. J. *Ibid.* **1982**, *104*, 4803. (e) Demas, J. N.; Taylor, D. G. *Inorg. Chem.* **1979**, *18*, 3177. (f) Gleria, M.; Minto, F.; Baggiato, G.; Bortolus, P. *J. Chem. Soc., Chem. Commun.* **1978**, 285.
(6) (a) Kober, E. M.; Meyer, T. J. *Inorg. Chem.* **1982**, *21*, 3978. Kober, E. M., Ph.D. Dissertation, University of North Carolina, 1982. (b) Hipps, K. W.; Crosby, G. A. *J. Am. Chem. Soc.* **1975**, *97*, 7042. (c) Hager, G. D.; Watts, R. J.; Crosby, G. A. *Ibid.* **1975**, *97*, 7037. (d) Ceulemans, A.; Vanquickenborne, L. G. *Ibid.* **1981**, *103*, 2238. (e) Daul, C. A.; Weber, J. *Chem. Phys. Lett.* **1981**, *77*, 593. (f) Belser, P.; Daul, C.; Von Zelewsky, A. *Ibid.* **1981**, *79*, 596.
(7) (a) Balzani, V.; Bolleta, F.; Gandolfi, M. T.; Maestri, M. *Top. Curr. Chem.* **1978**, *75*, 1. (b) Sutin, N.; Creutz, C. *Pure Appl. Chem.* **1980**, *52*, 2717. (c) Sutin, N. *J. Photochem.* **1979**, *10*, 19.
(8) (a) Hoggard, P. E.; Porter, G. B. *J. Am. Chem. Soc.* **1978**, *100*, 1457. (b) Wallace, W. M.; Hoggard, P. E. *Inorg. Chem.* **1980**, *19*, 2141. (c) Van Houten, J.; Watts, R. J. *Ibid.* **1978**, *17*, 3381.

0002-7863/83/1505-5583$01.50/0

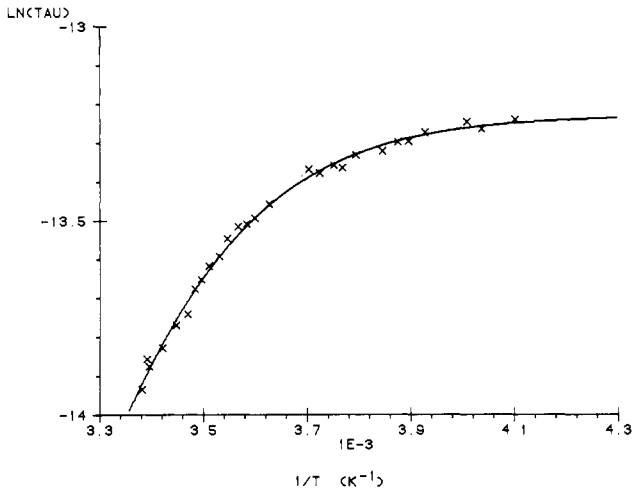

Figure 1. Plot of ln $[\tau(T)]$ vs. $1/T$ for $[Ru(bpy)_3](PF_6)_2$ in CH_3CN solution. The solid curve is the theoretical curve fit to the data with use of the expression for $\tau(T)$ given in eq 1 and the values of the parameters in Table I.

radiative and nonradiative decay of MLCT excited states and how they affect the transition between MLCT and d–d excited states.

Experimental Section

Materials. $[Ru(bpy)_3](PF_3)_2$ was prepared by the reaction of $RuCl_3 \cdot xH_2O$ and excess bpy in 1:1 $EtOH/H_2O$ at reflux for 3 h followed by precipitation with aqueous NH_4PF_6. The complex was purified by column chromatography on alumina with acetonitrile/toluene (1:1 v/v) as eluant, followed by recrystallization from acetonitrile/toluene. All solvents were of spectroscopic grade (Burdick-Jackson Laboratories) and were used as received. Solutions for use in lifetime and emission studies were bubble degassed for 20 min with purified argon.

Spectra. Emission spectra were recorded at 23 ± 2 °C on an SLM Instruments 8000 Photon Counting Spectrofluorimeter. Corrections for detector sensitivity were made with use of data and programs supplied with the instrument.

Emission Lifetimes. Emission lifetimes were determined by flash photolysis with excitation provided by the defocused 337-nm output from a pulsed Molectron Corp. nitrogen laser (pulse width ~ 10 ns). The luminescence intensity at the wavelength of the emission maximum was monitored as a function of time following excitation with use of an RCA1P28 photomultiplier tube attached to a Bausch & Lomb 33-86-02 monochrometer set at a right angle to the excitation pulse. Stray UV light was removed by 5 cm of nitromethane placed between the monochromator and the sample. The photomultiplier output was dropped across a 47-Ω resistor into the input stage of a Tektronix R7912 Transient Digitizer, which transferred the acquired waveform to a PDP 11/34 minicomputer. For lifetime determinations, 150 waveforms were acquired and averaged, and then fit to a simple first-order kinetic decay equation to obtain the observed luminescence lifetime, τ.

Temperature-dependent lifetimes were obtained with use of an Oxford Instruments Liquid Nitrogen Cryostat. Samples were degassed and sealed in 0.25 in. diameter Pyrex tubes. Solutions were kept dilute (~10^{-5} M) in order to prevent any precipitation of complex at low temperatures. The error in temperature measurements was estimated to be ±0.5 K. All lifetimes were acquired at temperatures above the freezing point of the solvent in order to avoid complications from phase transitions and lifetime variations induced by differences between phases.

Data Analysis. Temperature-dependent lifetimes were fit to the expression in eq 1 ($k = k_r + k_{nr}$) with use of a nonlinear least-squares procedure utilizing the Gauss–Newton algorithm.[5d]

$$\frac{1}{\tau(T)} = k + k'^0 \exp[-(\Delta E'/RT)] \quad (1)$$

Emission Quantum Yields. Radiative quantum yields, ϕ_r, were measured in deaerated (Ar bubbling, 20 min) solution at 25 ± 1 °C with use of $[Ru(bpy)_3](PF_6)_2$ in H_2O as a standard ($\phi_r = 0.042$).[5c] Corrections were made for differing refractive indices of the solvents as shown in eq 2,[10] where $\phi_r^{obs_d}$ is the uncorrected emission quantum yield, n is the refractive index of the solvent, and n_{H_2O} is the refractive index of water.

$$\phi_r = \phi_r^{obsd}\left(\frac{n^2}{n^2_{H_2O}}\right) \quad (2)$$

Table I. Excited State Decay Parameters for $Ru(bpy)_3^{2+}$ in a Variety of Solvents. The Values were Obtained by Fitting the Observed Temperature Dependence of the Luminescence Lifetime to the Expression in eq 1[a]

solvent	τ(25 °C) (μs)	$k = k_{nr} + k_r$ ($s^{-1} \times 10^{-5}$)	k'^0 ($s^{-1} \times 10^{-13}$)	$\Delta E'$ (cm^{-1})
dichloromethane	0.488	4.1	4.5	3560
n-butyronitrile	0.918	5.2	0.26	3140
pyridine	0.920	5.3	0.26	3180
acetonitrile	0.855	5.6	5.8	3800
propylene carbonate	0.938	6.1	0.35	3270
N,N-dimethylformamide	0.912	7.2	4.0	3820
water[b]	0.630	12.9	1.0	3560

[a] Error limits are: τ, k = ±2%; k'^0 = ±10–20%; $\Delta E'$ = ±25–50 cm^{-1}. Uncertainties for the k'^0 and $\Delta E'^0$ values were obtained from the Gauss–Newton algorithm fitting procedure used to analyze the temperature-dependent lifetime data. [b] Data from ref 5c.

Table II. Solvent Dependence of the Decay Properties of the $Ru(bpy)_3^{2+}$ MLCT Excited State at 25 °C[a]

solvent	E_{em} ($cm^{-1} \times 10^{-3}$)	fwhm[b] (cm^{-1})	ϕ_r	k_r ($s^{-1} \times 10^{-4}$)	k_{nr} ($s^{-1} \times 10^{-5}$)
dichloromethane	16.50	2750	0.029	5.9	3.5
n-butyronitrile	16.26	2890	0.060	7.5	4.4
pyridine	16.21	2780	0.042	4.7	4.8
acetonitrile	16.13	2870	0.062	7.7	4.8
propylene carbonate	16.05	2860	0.071	8.0	5.2
N,N-dimethylformamide	15.87	2940	0.063	7.2	6.4
water	15.97	3030	0.042[c]	6.9[c]	12.2[c]

[a] Estimated errors are as follows: E_{em} = ±50 cm^{-1}; fwhm = ±100 cm^{-1}; ϕ_r = ±10%; k_r = ±15%; k_{nr} = ±4%. [b] Full width at half maximum of the emission band. [c] Data from ref 5c.

Values of the radiative (k_r) and nonradiative (k_{nr}) decay rate constants for the MLCT excited states were determined from the experimental values of $\tau(T)$ and ϕ_r by using eq 3 and 4.

$$k_r = \phi_r \tau^{-1} \quad (3)$$

$$k_{nr} = k - \phi_r \tau^{-1} \quad (4)$$

Results

In Figure 1 is shown a plot of ln (τ) as a function of temperature in acetonitrile solution. The solid curve represents the calculated fit of the data with use of the expression for $\tau(T)$ given in eq 1 and a Gauss–Newton algorithm fitting procedure provided by Tektronix and available in the "Tektronix Handshake Application Program Library", Tektronix Corp., Beaverton, OR. The values of k, k'^0, and $\Delta E'$ obtained from fits of this type in a series of different solvents are presented in Table I. It is important to realize that although variations in room-temperature lifetimes between solvents are relatively small, k'^0 and $\Delta E'$ are well-defined. The reason is that k'^0 and $\Delta E'$ values were obtained from an analysis of temperature-dependent lifetimes based on from 21 to 46 different temperatures. The extent of data taken depended largely on the liquid range of the solvent.

The results of the measurement of the solvent dependence of ϕ_r for $Ru(bpy)_3^{2+}$ are presented in Table II, together with the observed emission energy maxima, full width at half maximum for the emission bands, and calculated radiative and nonradiative decay rate constants for the MLCT → ground-state transition. Notice that the values of k_r are relatively solvent independent and that there are no apparent systematic variations in k_r with emission energy. On the other hand, values for k_{nr} increase as the emission energy decreases.

Typical corrected emission spectra for $Ru(bpy)_3^{2+}$ in two different solvents are shown in Figure 2. Note that the band shapes are not affected greatly by solvent. The major effect of solvent variation is to change the energy of the emission maximum, although small variations in the full width at half maximum are also observed (see Table II).

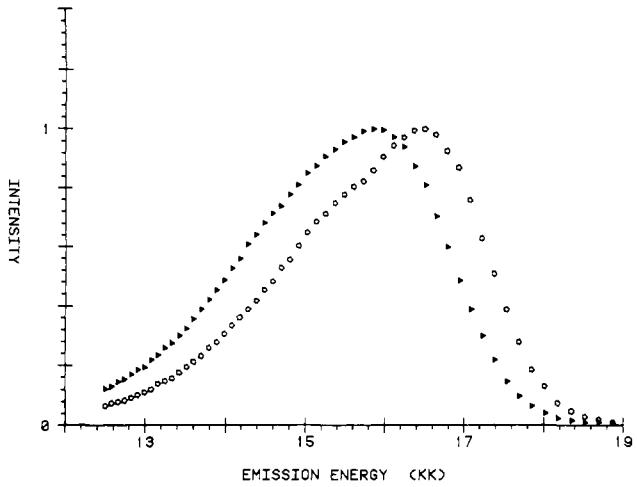

Figure 2. Emission spectra for $[Ru(bpy)_3](PF_6)_2$ in DMF (Δ) and CH_2Cl_2 (○) solution at 25 °C. The spectra have been corrected for detector sensitivity.

Discussion

A full accounting of the effect of solvent on the emission lifetime of $Ru(bpy)_3^{2+*}$ requires a complex analysis. From emission yield and temperature-dependent lifetime studies, the lifetime of the excited state is determined by rate terms for three separate processes from two different states: (1) radiative decay (k_r) and nonradiative decay (k_{nr}) from a low-lying MLCT state or states to the ground state, and (2) thermal activation to a d–d state or states which subsequently undergo decay to the ground state or photochemistry via ligand loss. As a consequence, in order to separate the experimentally observed solvent effect into contributions from the three separate processes, it is necessary to obtain emission yield and temperature-dependent lifetime data in a series of solvents. Having obtained the data it is possible to discuss the solvent dependence of each process in turn in the light of available theory.

The Effect of Solvent on Radiative and Nonradiative Decay of the MLCT State(s). From the results of low-temperature lifetime and emission-yield experiments of Crosby et al.[5a] the emitting state of $Ru(bpy)_3^{2+}$ actually consists of a manifold of three closely spaced ($\sim$100 cm^{-1}) states. At 200 K and higher each of the states are populated and contribute to excited-state decay. The results of a parameterized theoretical analysis[6a] show that the three low-lying states are largely triplet in character but can acquire singlet character through the effect of spin–orbit coupling. The state that is highest in energy of the three has the greatest singlet character and is expected to dominate both radiative and nonradiative decay even at temperatures well below ambient. Since all of the states have the same basic electronic configuration, $d\pi^5(Ru)\pi^*(bpy)$, there is no reason to believe that changes in solvent should change the ordering of the states.

There is by now good spectroscopic evidence that in the MLCT excited states the excited electron is localized on a single bpy ligand.[11] As a consequence of charge localization, there is an appreciable intramolecular charge transfer component that exists for excited-state decay, $(bpy^{-\cdot})Ru^{III}(bpy)_2^{2+*} \rightarrow Ru^{II}(bpy)_3^{2+}$, which provides a basis for solvent effects.

The results in Table II include values for k_r which were calculated from eq 3, $k_r = \phi_r/\tau$. Equation 3 is only correct if the efficiency of population of the emitting MLCT state(s) is unity. Absorption is dominated by transitions to MLCT states largely singlet in character and including the intersystem crossing efficiency, η_{isc}, gives $k_r = \phi_r/\eta_{isc}\tau$. Earlier work by Demas and Taylor[5e] in fluid solution at or near room temperature has shown that $\eta_{isc} = 1$ in methanol and in water, over a wide range of excitation wavelengths. However, in the range of solvents used here, deviations from unity may occur for η_{isc} and thus the values for k_r in Table II are really values of $\eta_{isc}k_r$. Since the radiative efficiencies are relatively low and do not exceed 8%, the effect of any such corrections on calculated values for k_{nr} should be negligible; note eq 4.

From the data for k_r (or $\eta_{isc}k_r$) in Table II, k_r is relatively insensitive to variations in solvent. This is an expected result since the Einstein A coefficient for spontaneous emission predicts that k_r should vary as the cube of the emission energy if the dipole

$$k_r = \left(\frac{4E_{em}^3}{3\hbar^4c^3}\right)\mu_{12}^2$$

moment matrix element for the transition (μ_{12}^2) is constant. Since the observed range of values of E_{em} here is rather small, the predicted variation in k_r only amounts to ca. 20%. The near constancy of values of k_r in Table II also strongly suggests that significant variations in η_{isc} between solvents does not occur.

It is possible to consider the effects of solvent upon k_{nr} on the basis of the energy-gap law for radiationless transitions.[13] The energy-gap law is given in eq 5 in the form derived by Englman, Freed, and Jortner.[14,15] Equation 5 is valid in the high-temperature ($\hbar\omega_M \ll k_BT$), weak-vibrational coupling ($|\Delta E|/S_M\hbar\omega_M \gg 1$) limits.

$$k_{nr} = (C^2\omega_k)\left(\frac{\pi}{2\hbar\omega_M|\Delta E_k|}\right)^{1/2}\exp(-S)\exp\left(\frac{-\gamma|\Delta E_k|}{\hbar\omega_M}\right) \quad (5)$$

ΔE is the internal energy difference between the thermally equilibrated ground and excited states. As defined in this paper, $\Delta E < 0$ and the energy released on excited-state decay is ΔE. $|\Delta E_k| = |\Delta E| - \hbar\omega_k \approx |\Delta E|$ (for $\hbar\omega_k \ll |\Delta E|$) where ω_k is the angular frequency for the promoting vibration or vibrations; note below. $\omega_M = 2\pi\nu_M$, the angular frequency of the acceptor or deactivating vibration or vibrations. C^2 is the nuclear momentum matrix element for the promoting vibration of angular frequency ω_k which leads to the transition between states. The promoting vibration or vibrations are expected to be low-frequency vibrations which when excited lead to enhanced electronic overlap between the electron donor and acceptor sites. $S = {}^1/_2\sum_j\Delta_j^2$; Δ_j is the dimensionless fractional displacement of normal mode j between the equilibrium configurations of the ground and excited states. In terms of the equilibrium positions of the ground and excited states along the jth normal mode (Q_0^g and Q_0^e; in cm), $\Delta_j = (Q_0^g - Q_0^e)(M\omega_j/\hbar)^{1/2}$ where m is the reduced mass for the mode and ω_j is its vibrational frequency. In the limit of a single acceptor vibration, M, $S = S_M = {}^1/_2\Delta_M^2$. $\gamma = \ln(|\Delta E_k|/\hbar\omega_M S_M) - 1$.

Making the substitutions $\Delta E_k \approx \Delta E$ and $S = S_M$, eq 5 in logarithmic form becomes

$$\ln k_{nr} = \ln\beta - S_M - \left(\frac{\gamma|\Delta E|}{\hbar\omega_M}\right) \quad (6a)$$

$$\beta = C^2\omega_k\left(\frac{\pi}{2\hbar\omega_M|\Delta E|}\right)^{1/2} \quad (6b)$$

Although ΔE appears both in β and γ in eq 6, in the range of interest here both are slowly varying functions of ΔE compared with the term $\gamma\Delta E/\hbar\omega_M$ and eq 6 predicts that $\ln k_{nr}$ should vary linearly with ΔE.

The assumption of a single acceptor vibration or a closely spaced series of acceptor vibrations is supported by low-temperature

(9) Figgis, B. N. "Introduction to Ligand Fields"; John Wiley and Sons: New York, 1966.
(10) Demas, J. N.; Crosby, G. A. *J. Phys. Chem.* **1971**, *75*, 991.
(11) (a) Bradley, P. G.; Kress, N.; Hornberger, B. A.; Dallinger, R. F.; Woodruff, W. H. *J. Am. Chem. Soc.* **1981**, *103*, 7441. (b) Strukl, J. S.; Walter, J. L. *Spectrochim. Acta, Part A* **1971**, *27A*, 209. (c) Strukl, J. S.; Walter, J. L .*Ibid.* **1971**, *27A*, 223.
(12) This result is based on the Einstein coefficient for spontaneous emission. See, for example: Steinfield, J. I. "Molecules and Radiation: An Introduction to Modern Molecular Spectroscopy"; MIT Press: Cambridge, Mass., 1978.
(13) Siebrand, W. J. *Chem. Phys.* **1966**, *48*, 2732.
(14) Englman, R.; Jortner, J. *Mol. Phys.* **1970**, *18*, 145.
(15) Freed, K. F.; Jortner, J. *J. Chem. Phys.* **1970**, *52*, 6272.

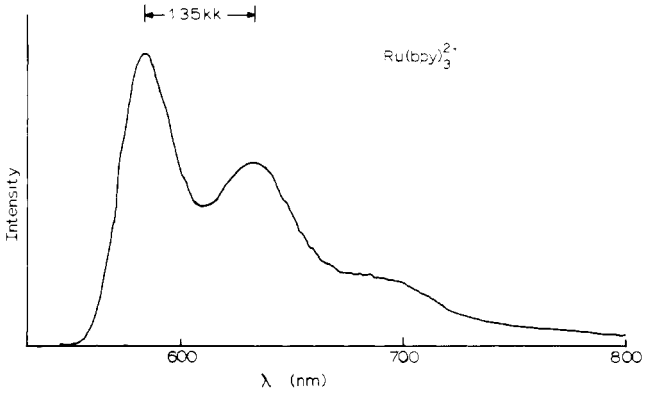

Figure 3. Emission spectra for $[Ru(bpy)_3](PF_6)_2$ in 4:1 EtOH/MeOH glass at 77 K. The spectrum has been corrected for detector sensitivity.

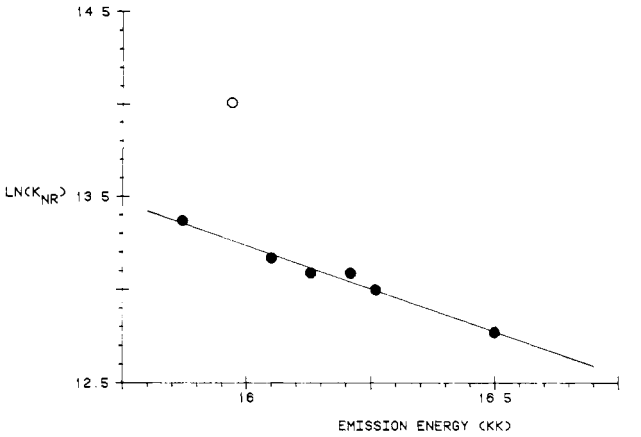

Figure 4. Plot of ln k_{nr} vs. E_{em} for $[Ru(bpy)_3](PF_6)_2$ in a series of nonhydroxylic solvents (●) and in H_2O (○).

emission spectra of $Ru(bpy)_3^{2+*}$ (Figure 3) and related excited states of Ru(II) and Os(II)[2,5a,17] which are dominated by a single high frequency vibrational progression with $\hbar\omega_M \sim 1300$–1400 cm^{-1}. The vibrations in this region are bpy-localized framework in nature[2,11] which are expected to respond ($\Delta_M^2 \neq 0$) to the change in electronic configuration between excited and ground states, $(bpy^{-}\cdot)Ru^{III} \rightarrow (bpy)Ru^{II}$.

Excited-state decay corresponds to a transition between different eigenstates. Because of the orthogonality of the states, such transitions are ostensibly forbidden but can be induced by excitation of normal vibrations which lead to changes in overlap between the electron-donor and -acceptor sites. With the assumption of single such "promoting" vibration, C^2 has the form shown in eq 7 where ψ_g and ψ_e are the ground- and excited-state

$$C^2 \propto \left|\left\langle \psi_g \left| \frac{\partial}{\partial Q_k} \right| \psi_e \right\rangle\right|^2 \quad (7)$$

electronic wavefunctions and $\partial/\partial Q_k$ is the nuclear momentum operator for the promoting vibration. Given the electronic nature of the MLCT excited-state decay process, low-frequency, metal–ligand stretching and bending vibrations are expected to dominate the role of promoting vibrations.[6a] Given its origin, it would not be surprising if the term $C^2\omega_k$ were relatively independent of solvent.

As it stands, eq 7 does not explicitly include contributions from lower frequency, intramolecular vibrations ω_L, nor from the collective, low-frequency vibrations of the solvent, ω_0. Including the solvent in the high-temperature limit, $\hbar\omega_0 \ll k_BT$, and a contribution from a lower-frequency intramolecular vibration, leads to eq 8.[3]

$$\ln k_{nr} = \ln \beta_0 - S_M - \frac{\gamma_0(|\Delta E| - \chi_0)}{\hbar\omega_M} + \frac{\chi_0}{\hbar\omega_M}\left[\frac{k_BT}{\hbar\omega_M}(\gamma_0 + 1)^2\right] + S_L\left(\frac{\omega_L}{\omega_M}\right)(\gamma_0 + 1) \quad (8)$$

$\chi_0 = S_0\hbar\langle\omega_0\rangle$; the classical solvent vibrational trapping energy where $\langle\omega_0\rangle$ is an averaged frequency for the low-frequency collective vibrations of the solvent and S_0 is related to the corresponding fractional displacement between thermally equilibrated ground and excited states by $S_0 = {}^1/_2\Delta_0^2$. $\gamma_0 = \ln((|\Delta E| - \chi_0)/S_M\hbar\omega_M) - 1$. $\beta_0 = C^2\omega_k[\pi/(2\hbar\omega_M(|\Delta E| - \chi_0))]^{1/2}$. S_L, ω_L are the angular frequency and fractional displacements for vibration L. Equation 8 is appropriate for the limiting case of contributions only from the lowest ($\omega_L = 0$) vibrational level in the excited state.

In order to be able to use eq 8 experimentally, it is convenient to re-write it in terms of the emission energy, which is a measurable quantity. The relationship between ΔE and $E_{em}(0\text{–}0)$, the energy of the $\nu'_M = 0$ vibrational component of the emission manifold, is given in eq 9 in terms of the 0–0 ($\nu_M = 0$, $\nu_L = 0$) emission energy, $E_{em}(0\text{–}0)$. In general, it is not possible to measure

$$|\Delta E| = E_{em}(0\text{–}0) + \chi_0 \quad (9)$$

$E_{em}(0\text{–}0)$ at room temperature because of temperature-induced broadening of the individual vibrational components in the emission spectrum.[19] Thermal broadening at high temperature leads to extensive overlap of the individual components, giving rise to broad, structureless emission bands. However, in the limit of relatively slight excited-state distortion, $S_M < 1$, $E_{em}(0\text{–}0) \approx E_{em}$, where E_{em} is energy at the maximum intensity in the room-temperature emission spectrum. As will be discussed in a forthcoming paper, there is evidence for contributions to the 77 K emission spectra from low-frequency ν(RuN) vibrations. However, their contributions to room-temperature spectra are negligible.

As discussed in Appendix I, for $Ru(bpy)_3^{2+*}$, fits of the observed room-temperature emission spectra show that E_{em} and $E_{em}(0\text{–}0)$ are related linearly by eq 10 where $a = 1.03$ and $b = 850$ cm^{-1}.

$$E_{em} = aE_{em}(0\text{–}0) - b \quad (10)$$

The use of the relationship $E_{em} \approx E_{em}(0\text{–}0) - b$ first in eq 9 and then in eq 8 gives rise to eq 11 which is of considerable utility

$$\ln k_{nr} = \left(\ln \beta_0 - \frac{b\gamma_0}{\hbar\omega_M} - S_M\right) - \frac{\gamma_0 E_{em}}{\hbar\omega_M} + \frac{\chi_0}{\hbar\omega_M}\left[\frac{k_BT}{\hbar\omega_M}(\gamma_0 + 1)^2\right] + S_L\left(\frac{\omega_L}{\omega_M}\right)(\gamma_0 + 1) \quad (11)$$

experimentally because it is written in terms of the room-temperature emission energy, which removes the necessity of obtaining $E_{em}(0\text{–}0)$ from spectral fitting. Equation 11 can be further simplified in form by noting that for $Ru(bpy)_3^{2+*}$, the term $(k_BT/\hbar\omega)(\gamma_0 + 1)^2 \sim 1.0$ which gives eq 12.

$$\ln k_{nr} = \left(\ln \beta_0 - \frac{b\gamma_0}{\hbar\omega_M} - S_M + S_L\left(\frac{\omega_L}{\omega_M}\right)(\gamma_0 + 1)\right) - \frac{\gamma_0 E_{em}}{\hbar\omega_M} + \frac{\chi_0}{\hbar\omega_M} \quad (12)$$

Equations 11 or 12 predict that ln k_{nr} should vary linearly with E_{em}, a result that we have previously verified experimentally by using a series of related chromophores in a constant solvent.[2,3] However, if variations in E_{em} are induced by variations in solvent, a linear relationship is expected only if variations in χ_0 are small compared to variations in $\gamma_0 E_{em}$. In Figure 4 is shown a plot of ln k_{nr} vs. E_{em} for $Ru(bpy)_3^{2+*}$ in a series of solvents. Clearly the

(16) Lin, S. H. *J. Chem. Phys.* **1966**, *44*, 3759.
(17) Caspar, J. V., Ph.D. Thesis, University of North Carolina, 1982, and unpublished results.
(18) Hush, N. S. *Electrochim. Acta* **1968**, *13*, 1005; *Prog. Inorg. Chem.* **1967**, *8*, 391.
(19) Ballhausen, C. J. "Molecular Electronic Structures of Transition Metal Complexes"; McGraw-Hill: New York, 1979.

Table III. Slopes and Intercepts Observed from Plots of ln k_{nr} vs. E_{em} for the Emitting MLCT Excited States of $Ru(bpy)_3^{2+}$ and $Os(bpy)L_4^{2+}$ [a]

	slope (eV^{-1})	intercept
$Ru(bpy)_3^{2+}$ [b]	−7.4 ± 0.7	28.0 ± 1.1
$Os(bpy)L_4^{2+}$ [c]	−7.5 ± 0.7	29.2 ± 1.1

[a] The uncertainties cited represent the 95% confidence level from a least-squares error analysis. [b] Data obtained for $Ru(bpy)_3^{2+}$ decay in a series of solvents. [c] Data obtained for a series of different complexes in CH_3CN solution. See ref 2.

predicted linear relationship is observed for the nonhydroxylic solvents used in the correlation in Figure 4, which suggests that variations in χ_0 with solvent may be relatively small. However, in Figure 4 the point for water lies well off the line and the apparent deviation associated with water as solvent will be discussed below.

As noted above, plots of ln k_{nr} vs. E_{em} for the MLCT excited states of the series of complexes $Os^{II}(bpy)L_4^{2+}$ (L = $^1/_2$bpy, $^1/_2$phen, PR_3, CH_3CN, Me_2SO, AsR_3, etc.)[2] in a common solvent, CH_3CN, are also linear as predicted by eq 11. For the Os(II) complexes, the $d\pi(Os(II)) \rightarrow \pi^*(bpy)$ chromophore remains constant, and variations in ΔE and E_{em} are induced by variations in the ligands L rather than by variations in solvent.

In Table III are given the experimental slopes and intercepts from plots of ln k_{nr} vs. E_{em} for the two different types of experiments. It is striking that within experimental error the slopes are identical. The small difference in intercepts between the two different types of experiments with the higher intercept for Os is probably meaningful. From eq 11, the intercept includes among other factors the term C^2. From eq 7, the magnitude of C^2 depends on electronic overlap terms which are expected to have a greater magnitude for Os than for Ru. The origin of the increase in C^2 for Os is in the greater spin–orbit coupling constant for Os compared to Ru, $\lambda_{Os} \sim 3\lambda_{Ru}$. With greather spin–orbit coupling, the extent of mixing between the ^{3}MLCT and low-lying MLCT singlet states is greater. Since the ground state is largely singlet in character, the magnitude of the integral for C^2 in eq 7 will increase as the singlet character of ψ_e increases. This increase is a direct result of the fact that operator $\partial/\partial Q_k$ is not a function of spin.

The agreement between slopes for the two different types of experiments leads to a number of important conclusions: (1) Nonradiative decay from the MLCT excited state(s) of $Ru(bpy)_3^{2+}$ can be understood quantitatively on the basis of the underlying assumptions of the energy gap law. (2) The ν(bpy) acceptor vibration(s) with $\hbar\omega_M \sim 1300$–1400 cm^{-1} remain the same for $Ru(bpy)_3^{2+*}$ and for the Os^{II}-bpy MLCT excited states. (3) For the polar organic solvents which define the linear relationship in Figure 4, variations in χ_0 must be small compared to the variations in $\gamma_0 E_{em}$. (4) In comparing the two experiments, the term γ (= ln $(|\Delta E|/S_M\hbar\omega_M) - 1$) in eq 6 or γ_0 (= ln $(E_{em}/S_M\hbar\omega_M) - 1$) in eq 11 must be constant or vary in the same way with ΔE. As noted in Appendix I, S_M can be evaluated from a Franck–Condon analysis of the relative intensities of vibrational progressions observed in emission spectra. With use of the analysis in Appendix I, for the series of Os-bpy complexes, low-temperature (77 K) experiments in 4:1 EtOH/MeOH glasses show that S_M increases with E_{em}. The linear relationship between ln k_{nr} and E_{em} is maintained because γ_0 also varies linearly with E_{em}.[22] In order for the solvent-dependence experiment reported here to give the same slope, the sense of the variation of S_M with E_{em} must remain the same even though the changes in excited-state distortion are induced by variations in solvent rather than in the ligand L. Qualitatively, such a conclusion can be reconciled on the basis of the following argument: (1) As E_{em} (and $|\Delta E|$) increase, regardless of the origin of the increase, the separation between ground and excited states increases. (2) As the energy gap between states increases, the extent of excited-state mixing into the ground state decreases and the extent of charge transfer in forming the excited state increases. (3) As the extent of charge transfer increases, the extent to which the coordinated bpy is reduced in the excited state increases and hence the extent of excited-state distortion along the deactivating vibration increases. In fact, a detailed accounting of the slopes of plots of ln k_{nr} vs. E_{em} can be made on the basis of systematic variations in S_M and S_L values calculated from low-temperature emission spectra. This subject will be the theme of a forthcoming publication.

As noted above, the data in Figure 4 suggest that a "special" effect must exist for water. Other experiments have shown that the origin of the effect for the Os(II) MLCT excited states lies in non-negligible differences in χ_0 between typical polar organic solvents and hydroxylic solvents like H_2O or CH_3OH, with H_2O having the most dramatic effect.[16] It is also obvious from the magnitudes of kinetic isotope effects in O–H for deuterated solvents that a complete accounting of the "special" effects for hydroxylic solvents is not accessible from dielectric continuum theory. We are currently investigating the origin of solvent effects and how they determine the magnitudes of E_{em} and χ_0.

Solvent Effects on the Transition between MLCT and d–d Excited States. The third solvent-dependent kinetic term which determines the photophysical properties of $Ru(bpy)_3^{2+*}$ is the temperature-dependent term in eq 1. It should be noted that the fitting procedure that we utilized assumed that all of the temperature dependence in the experimental lifetimes appears in the exponential term in eq 1. That the treatment is adequate is shown clearly by the agreement between the experimental and calculated curves in Figure 1. In fact, experiments with osmium(II) polypyridyl complexes where there are no complications from dd states show that a slight temperature dependence also exists for k_{nr} but that the effect is sufficiently small as to be negligible here. The origin of the dependence is in the energy gap law (eq 12), through the variation of E_{em} with temperature which causes a temperature dependence in k_{nr}.

The temperature-dependent term in eq 1 has been attributed to the thermally activated population of a d–d excited state followed by decay or photochemical ligand loss.[5d,8c] It is apparent from the data in Table I that both the pre-exponential (k'^0) and exponential ($\Delta E'$) components of the temperature-dependent term vary significantly with solvent.

A kinetic scheme for population and decay of the d–d excited state is shown in the equation

$$\text{MLCT} \underset{k_{-2}}{\overset{k_2}{\rightleftharpoons}} \text{d–d} \qquad (13a)$$

$$\text{d–d} \xrightarrow{k_3} \text{ground state or photochemistry} \qquad (13b)$$

The constants in the scheme are related to the experimentally measured quantity $k' = k'^0 \exp(-\Delta E'/RT)$ as shown here

$$k' = k_2\left(\frac{k_3}{k_{-2} + k_3}\right) \qquad (14)$$

In the limit that $k_{-2} \gg k_3$, d–d excited-state decay is slow compared to repopulation of the MLCT state, the two states are in equilibrium, and eq 14 becomes

$$k' = k'^0 \exp(-\Delta E'/RT) = (k_2/k_{-2})k_3 \qquad (15)$$

In the other limit, $k_o \gg k_{-2}$, d–d excited-state decay is rapid, $\Delta E'$ is the energy of activation, and k'^0 is the pre-exponential term for MLCT → d–d surface crossing. In this limit eq 14 becomes

$$k' = k_2 = k^0 \exp(-\Delta E'/RT) = Aexp[-(E_a/RT)] \qquad (16)$$

Recent work based on lifetime studies in mixed chelates of Ru(II) suggests that examples of each limiting case of eq 14 may exist.[24]

(20) Herzberg, G. "Molecular Spectra and Molecular Structure"; Van Nostrand: New York, 1950; Vol. 1, Chapter 4.
(21) Yersin, H.; Otto, H.; Zink, J. I.; Gliemann, G. *J. Am. Chem. Soc.* **1980**, *102*, 951.
(22) Caspar, J. V.; Kober, E. M.; Sullivan, B. P.; Meyer, T. J., manuscript in preparation.
(23) Caspar, J. V.; Meyer, T. J., manuscript in preparation.

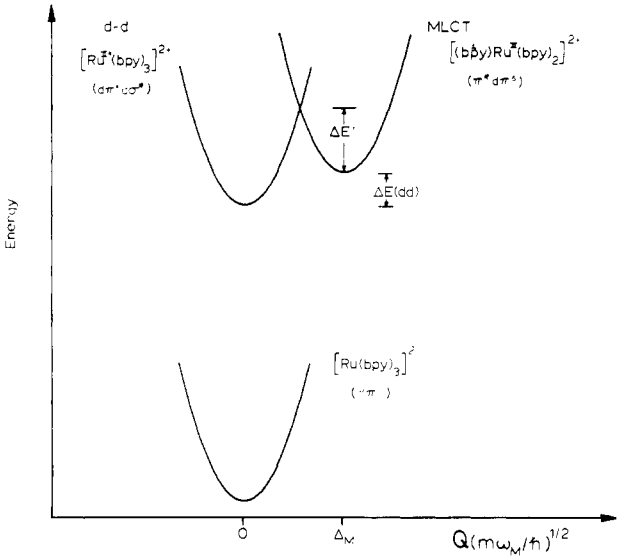

Figure 5. Schematic diagram showing variations in energy with fractional displacement relative to the ground state for the ν(bpy) acceptor vibration for the d–d and MLCT excited states for $Ru(bpy)_3^{2+}$. The variables that appear are defined in the text. Note that with regard to the *ligand-based (bpy) vibration* the figure shows that little distortion is expected to exist between the d–d and ground states but that the MLCT state is offset by Δ_M. Significant distortions between the d–d and ground states are expected along Ru–N normal coordinates.

For the first limiting case ($k_{-2} \gg k_3$) characteristic values of the measured kinetic parameters involving the d–d state are $k'^0 \sim 10^9$–10^{10} s^{-1} and $\Delta E' \sim 2000$ cm^{-1}. For the second case ($k_{-2} \ll k_3$), which appears to apply for $Ru(bpy)_3^{2+}$, $k^0{}_2 = k'^0$ is in the range 10^{12}–10^{14} s^{-1} and $\Delta E'$ is in the range 3000–4000 cm^{-1}.

With this interpretation, k' for $Ru(bpy)_3^{2+*}$ is the rate constant for the MLCT → d–d surface crossing. *The surface crossing (eq 17) can be viewed as a thermally activated ligand-to-metal*

$$MLCT((d\pi)^5(\pi^*(bpy)^1)) \xrightarrow{k_2} d\text{–}d((d\pi)^5(d\sigma^*)^1) \quad (17)$$

electron-transfer reaction with $E_a = \Delta E'$ (eq 16). The relationship between the d–d, MLCT, and ground-state energy curves is shown schematically in Figure 5. Note that Figure 5 is an energy-coordinate diagram for the ligand-based ν(bpy) acceptor vibration. As shown in the figure, it is expected that little distortion should exist between the d–d and ground states with regard to this coordinate, although the MLCT state is offset by Δ_M. Significant distortions between the ground and d–d excited states should obviously exist along Ru–N normal coordinates.

From a quantum mechanical treatment, the rate constant for a thermally activated electron-transfer reaction is given by eq 18

$$k_2 = k_{et} = \frac{2\pi V^2}{\hbar}\left(\frac{1}{16\pi k_B T \chi(dd)}\right)^{1/2} \exp\left[-\left(\frac{[\chi(dd) + \Delta E(dd)]}{4\chi(dd)k_B T}\right)\right] = \nu_{et}\exp[-E_a/RT] \quad (18)$$

$$\nu_{et} = \frac{2\pi V^2}{\hbar}\left(\frac{1}{16\pi k_B T \chi(dd)}\right)^{1/2}$$

$$\Delta E' = E_a(dd) = \frac{[\chi(dd) + \Delta E(dd)]^2}{4\chi(dd)} \quad (19)$$

$$k'^0 = A = \frac{2\pi V^2}{\hbar}\left[\frac{1}{16\pi k_B T \chi(dd)}\right]^{1/2}, \quad (20)$$

$$\chi(dd) = \chi_0(dd) + \chi_i(dd) \quad (21)$$

in the classical limit.[25] In eq 18–21 the intramolecular (χ_i(dd)/4) and solvent (χ_0(dd)/4) classical vibrational trapping energies, and the internal energy change on electron transfer (ΔE(dd)) associated with the MLCT → dd transition, are distinctly labeled to distinguish them from the related quantities (χ_i, χ_0, ΔE) used earlier to describe the nonradiative MLCT → ground state decay process.

For the MLCT → d–d transition there are expected to be significant contributions to χ_i(dd) from high-frequency ν(bpy) vibrations, as there are in k_{nr} for MLCT decay, and from lower-frequency ν(Ru–N) vibrations given the expected distortions in the $d\pi^5 d\sigma^*$ excited state. Equation 18 can be modified explicitly to accommodate such contributions.[25] However, the classical approximation used to derive eq 18 is appropriate for the low-frequency (1–10 cm^{-1}) collective trapping vibrations of the solvent. In eq 18 solvent-dependent terms appear in both the exponential (χ(dd) and ΔE(dd)) and pre-exponential (χ(dd)) terms. In the classical dielectric continuum limit, χ_0(dd) is given by the equation[18]

$$\chi_0(dd) = \frac{1}{2}\left(\frac{1}{D_{op}} - \frac{1}{D_s}\right)\int (\vec{E}_f - \vec{E}_i)^2\, dV \quad (22)$$

and ΔE(dd) by

$$\Delta E(dd) = \Delta E_g(dd) + \frac{1}{2}\frac{1}{D_s}\int (\vec{E}_f^2 - \vec{E}_i^2)\, dV \quad (23)$$

In eq 22 and 23, ΔE_g(dd) is the gas-phase component of ΔE(dd), $\vec{E}_i$ and $\vec{E}_f$ are the electric field vectors in the gas phase before and after electron transfer, D_{op} and D_s are the optical and static dielectric constants of the medium, and the integration is over the volume surrounding the ion or molecule.

Equation 18 provides a basis for discussing the solvent dependence of both the pre-exponential ($k'^0 = k_2{}^0 = (2.6 \pm 0.4) \times 10^{12}$ s^{-1} to $(5.8 \pm 0.8) \times 10^{13}$ s^{-1} from Table I) and exponential ($\Delta E' = E_a(dd) = (3140 \pm 50)$ cm^{-1} to (3820 ± 50) cm^{-1} terms. On the basis of the preceding analysis, the following conclusions are worth noting: (1) The solvent dependence of E_a(dd) comes from both χ_0(dd) and ΔE(dd). It seems reasonable to assume that the energy of the d–d state is relatively insensitive to solvent variations given the lack of significant radial redistribution between the ground ($d\pi^6$) and excited states ($d\pi^5 d\sigma^*$).[9] Consequently, it is expected that the energetics of the MLCT → d–d ($d\pi^5\pi^* \rightarrow d\pi^5 d\sigma^*$) and MLCT → ground state ($d\pi^5\pi^* \rightarrow d\pi^*$) transitions may well have similar solvent dependences, including similar values of χ_0.

(2) For the MLCT → ground state transition, we concluded in the previous section that variations in χ_0 were relatively small compared to variations in E_{em} for the series of non-hydroxilic, polar organic solvents. Given the conclusion reached in (1) above, variations in χ_0(dd) should also be small compared to variations in ΔE(dd). However, χ_0(dd) may be significant for hydroxylic solvents and especially for water, given the special effect of water in MLCT nonradiative, excited-state decay.

(3) Expanding eq 19 for the MLCT → dd transition gives

$$\Delta E' = E_a(dd) = \frac{\chi(dd)}{4} + \frac{\Delta E(dd)}{2}\left(1 + \frac{\Delta E(dd)}{2\chi(dd)}\right) \quad (24)$$

which points out the potential complexity of the solvent dependence of E_a(dd). In eq 24 the solvent appears through χ(dd)/4 *and* through terms which are linear and quadratic in ΔE(dd). On the basis of eq 24 expressions can be derived which relate E_a(dd) and E_{em}, but the scatter and imprecision in the data preclude a more detailed analysis.

(4) As can be seen by plotting the data in Table I, a linear correlation exists between k'^0 and $\Delta E'$, and from a linear least-

(24) Rillema, D. P.; Allen, G. H.; Meyer, T. J., manuscript in preparation.

(25) (a) Kestner, N. R.; Logan, J.; Jortner, J. *J. Phys. Chem.* **1974**, *78*, 1248. (b) Levich, V. G. In "Physical Chemistry: An Advanced Treatise"; Eyring, H., Henderson, D., Jost, W., Eds.; Academic Press: New York, 1970; Vol. 9B. (c) Soules, J. F.; Duke, C. B. *Phys. Rev. B: Solid State* **1971**, *B3*, 262. (d) Fischer, S. F.; Van Duyne, R. P. *Chem. Phys.* **1977**, *26*, 9.

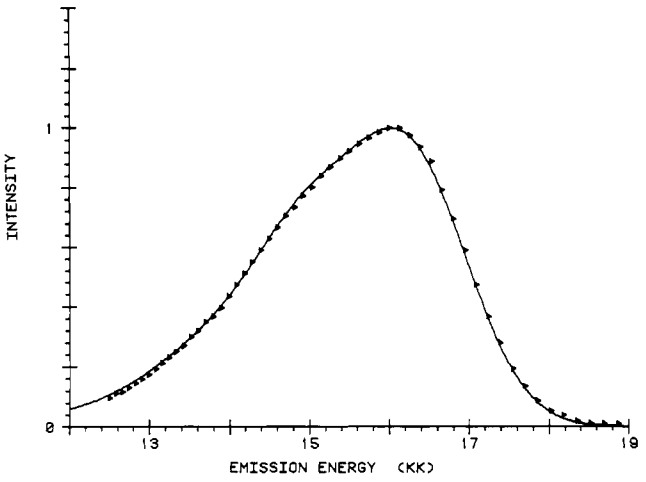

Figure 6. Corrected emission spectrum for $[Ru(bpy)_3](PF_6)_2$ in propylene carbonate at 25 °C (▲). The solid curve is the theoretical fit obtained by using eq A1 with $E_{em}(0\text{–}0)$ = 16 300 cm^{-1}, $\hbar\omega_M$ = 1350 cm^{-1}, S_M = 0.99, and $\nu_{1/2}$ = 1700 cm^{-1}.

squares analysis the slope of the line is 4.7×10^{-3} cm^{-1} with an intercept of 13.7. Similar relationships (Barclay–Butler plots)[28] have been observed previously in reactions involving solvent variations[29] although the data are usually presented as linear correlations between the activation parameters $T\Delta S^*$ and ΔH^* of reaction rate theory.[29c]

Implications of Solvent Effects for the Use of Ru(bpy)$_3^{2+*}$ as a Sensitizer. The MLCT excited state of $Ru(bpy)_3^{2+}$ has been used extensively as a photosensitizer because of its relatively long solution lifetime and its ability to act as either an electron-transfer acceptor or donor in photoredox applications.[7] One consequence of our work is that it establishes a considerable solvent dependence for the excited-state lifetime and partitions the effects between radiative, nonradiative, and MLCT → d–d decay channels. The net effect of solvent on the lifetime can be significant as shown by the data in Table I where τ at room temperature varies from 0.48 to 0.94 μs over a range in solvents from CH_2Cl_2 to propylene carbonate. The value of the analysis given here is both in identifying the solvent-dependent components of τ and in demonstrating that electron-transfer theory provides a useful basis for understanding the observed effects.

At 298 K, the MLCT → d–d transition represents a major decay pathway for all the solvents studied with the fraction of decay through this channel ranging from 0.37 in DMF to 0.80 in CH_2Cl_2. In photosensitization schemes, decay through the d–d state represents a major energy loss pathway since the d–d state appears to be short-lived, and there is at present no evidence that it undergoes redox quenching reactions. Another important aspect of decay through the MLCT → d–d decay channel is that previous studies have shown that the dd excited state is substitution labile,[5c,d,f,8c] and its population can lead to photodegradation. The efficiency of the observed photochemistry (ϕ_p) has been shown to be extremely solvent dependent, ranging from $\phi_p \leq 2.1 \times 10^{-5}$ in 0.1 M HCl[8c] to ϕ_p = 0.100 in CH_2Cl_2[5d,f] for $[Ru(bpy)_3]Cl_2$ at 298 K. It should be realized that the majority of the solvent effect on photosubstituion appears to be a consequence of the solvent-dependent chemistry of intermediates formed after the MLCT → d–d transition. Nonetheless, the accessibility of the d–d excited state(s) in $Ru(bpy)_3^{2+}$ and related complexes can represent a major drawback to their use as photosensitizers, and points to the need for new synthetic developments aimed at preparing related MLCT excited states where d–d states do not interfere with desired photochemical reaction pathways.

Table IV. Values of $E_{em}(0\text{–}0)$ Obtained from Fits of the $[Ru(bpy)_3](PF_6)_2$ 25 °C Emission Spectrum to the Expression in eq A1

solvent	$E_{em}(0\text{–}0)$ ($\times 10^3$ cm^{-1})
dichloromethane	16.75
n-butyronitrile	16.51
pyridine	16.49
acetonitrile	16.40
propylene carbonate	16.30
N,N-dimethylformamide	16.15

Acknowledgments are made to the National Science Foundation under Grant No. CHE-8008922 for support of this research.

Appendix I

The band shapes of the emission spectra can be calculated by using the expression in eq A1[20,21] which is valid for the case in which there is one high-frequency vibration or a series of closely spaced vibrations, ω_M, dominating the observed vibrational progressions. In eq A1, $I(E)$ is the emission intensity at energy E,

$$I(E) = \sum_{v=0}^{N} \left(\frac{E_{em}(0\text{–}0) - v\hbar\omega_M}{E_{em}(0\text{–}0)} \right)^4 \left(\frac{(S_M)^v}{v!} \right) \times \exp\left[-4 \log (2) \cdot \left(\frac{E - E_{em}(0\text{–}0) + v\hbar\omega_M}{\nu_{1/2}} \right)^2 \right] \quad \text{(A1)}$$

v is the vibrational quantum number of ground-state acceptor vibration ω_M, and $\nu_{1/2}$ is the full width at half maximum of an individual vibrational component. The term $([E_{em}(0\text{–}0) - v\hbar\omega_M]/E_{em}(0\text{–}0))^4$, which has its origin in the Einstein A coefficient for spontaneous emission, represents an important correction to the band shape which has been frequently omitted. For absorption an analogous term, $([E_{em}(0\text{–}0) - v\hbar\omega_M]/E_{em}(0\text{–}0))$, is also often neglected. In theory, the observed emission profile could be fit by eq A1 to obtain values of S_M, $\hbar\omega_M$, $\nu_{1/2}$, and $E_{em}(0\text{–}0)$. In practice a procedure of this type is not likely to be very accurate for the situation of interest here where the room-temperature bands are broad and unstructured. In our cases reasonable guesses can be made for $\hbar\omega_M$, S_M, and $\nu_{1/2}$ on the basis of the observed 77 K emission spectra and then these values can be refined to fit the room-temperature spectra. In estimating $\nu_{1/2}$ from 77 K spectra, the predicted linear dependence of $\nu_{1/2}$ on $T^{1/2}$ must be included.[19] Our procedure in fitting the room-temperature spectra was to fix the value of $\hbar\omega_M$ at the 77 K value of 1350 cm^{-1} and by using initial estimates of S_M = 1 and $\nu_{1/2}$ = 1700 cm^{-1} to fit the observed spectra by iteration to obtain the values of $E_{em}(0\text{–}0)$ shown in Table IV. As will be discussed in a forthcoming paper, there is evidence for contributions to the 77 K emission spectra from low-frequency ν(Ru–N) vibrations. However, their contributions to the room-temperature spectra are negligible. A typical fit of an experimental room-temperature spectrum is shown in Figure 6 for $Ru(bpy)_3^{2+}$ in propylene carbonate with $E_{em}(0\text{–}0)$ = 16 300 cm^{-1}, $\hbar\omega_M$ = 1350 cm^{-1}, S_M = 0.99, and $\nu_{1/2}$ = 1700 cm^{-1}. As expected, the values obtained for $E_{em}(0\text{–}0)$ are all blue shifted from the emission-energy maxima. The relationship between the emission energy, E_{em}, and $E_{em}(0\text{–}0)$, derived as described above, is given by

$$E_{em} = aE_{em}(0\text{–}0) - b$$

with a = 1.03 and b = 850 cm^{-1}. Since we are primarily interested in the slopes of plots of ln k_{nr} vs. $E_{em}(0\text{–}0)$, the small factor of 1.03 should be unimportant in influencing the results and the approximation $E_{em} \approx E_{em}(0\text{–}0) - b$ is reasonable. In comparing

(26) Geoffroy, G. L.; Wrighton, M. S. "Organometallic Photochemistry"; Academic Press: New York, 1979.
(27) (a) Marcus, R. A. *J. Chem. Phys.* **1965**, *43*, 1261. (b) Ulstrup, J. "Charge-Transfer Processes in Condensed Media"; Springer-Verlag: New York, 1979.
(28) Barclay, I. M.; Butler, J. A. V. *Trans. Faraday Soc.* **1938**, *34*, 1445.
(29) (a) Laidler, K. L. "Chemical Kinetics"; 2nd ed.; McGraw-Hill: New York, 1965; pp 46–47. (b) Gutierrez, A. R.; Adamson, A. W. *J. Phys. Chem.* **1978**, *82*, 903. (c) Leffler, J. E.; Grunwald, E. "Rates and Equilibria of Organic Reactions"; John Wiley: New York, 1963.
(30) See, e.g.: Jorgenson, C. K. "Absorption Spectra and Chemical Bonding in Complexes"; Pergamon Press: New York, 1962.
(31) Bock, C. R.; Connor, J. A.; Gutierrez, A. R.; Meyer, T. J.; Whitten, D. G.; Sullivan, B. P.; Nagle, J. K. *J. Am. Chem. Soc.* **1979**, *101*, 4815.

the results obtained here for $Ru(bpy)_3^{2+}$ to our earlier results obtained for $Os(bpy)L_4^{2+}$, values of E_{em} have been used since the dependence of $E_{em}(0-0)$ on E_{em} is very similar for both systems. As a result of the substitution of E_{em} for $E_{em}(0-0)$, the absolute values of the intercepts of plots of ln k_{nr} vs. E_{em} will be shifted by an amount $-b\gamma_0/\hbar\omega_M$ from those observed when ln k_{nr} is plotted against $E_{em}(0-0)$. Since the magnitude of b is comparable for $Ru(bpy)_3^{2+}$ and $Os(bpy)L_4^{2+}$, the magnitude of the difference in the intercepts, which can be related to the difference in the vibrationally induced electronic coupling term C^2 for the Ru and Os excited states, will be unaffected by the substitution of E_{em} for $E_{em}(0-0)$.

Registry No. $Ru(bpy)_3^{2+}$, 15158-62-0; dichloromethane, 75-09-2; *n*-butyronitrile, 109-74-0; pyridine, 110-86-1; acetonitrile, 75-05-8; propylene carbonate, 108-32-7; *N,N*-dimethylformamide, 68-12-2.

Supplementary Material Available: Tables of the temperature dependence of the excited-state lifetime of $[Ru(bpy)_3](PF_6)_2$ in the six solvents used in this study (6 pages). Ordering information is given on any current masthead page.

Distribution of Site Reactivities in Photoreactive Amorphous Solids

Eric Pitts and Arnost Reiser*

Contribution from the Research Division, Kodak Limited, Headstone Drive, Harrow, Middlesex HA1 4TY, England. *Received June 16, 1982*

Abstract: The kinetics of photoprocesses in amorphous solids are determined by the distribution of reactivities over an ensemble of matrix sites. A method is described which allows the estimation of reactivity distributions from the dependence of the macroscopic quantum yield of the photoreaction on the degree of reactant conversion. The procedure is illustrated on three industrial photopolymers and is shown to provide in this instance a useful insight into the molecular mechanism of cross-link formation.

In recent years the photochemistry of amorphous solids has attracted attention partly because of the industrial uses of solid-state photochemistry[1-3] and partly because of the information provided by photochemical probes into the structure and the molecular dynamics of solid polymers.[4-14]

In the solid phase, the environment of a reactant influences the chemical process by its physical presence or by direct participation in the chemistry. The reactant cannot, therefore, be considered in isolation, but it must be taken together with its immediate surroundings.[15,16] This approach leads to the concept of reactant sites and to a view of the photoreactive matrix as an ensemble of such sites.

On a molecular scale the ensemble of chromophore sites may be described by a distribution of site properties. If the distribution function of a particular site property is known, the corresponding macroscopic property of the solid may be derived from it. Property distributions exist in all unordered systems, but there is in this respect a fundamental difference between fluids and solids: in fluids, time averaging ensures the approximate constancy of the distribution, so that these systems can be treated as if they consisted of identical molecules of unchanging average properties. In solids, by contrast, the distribution of site properties may change drastically in the course of the chemical process, and with it property averages and the macroscopic behavior of the system. The distribution of site properties in a solid matrix is therefore of practical interest.

This paper is concerned with site reactivities. Their distribution determines the overall photokinetic behavior of the solid and as a consequence it should be possible to determine reactivity distributions from experimentally observed reaction rates. Kryszewski et al.[17] were the first to show how an inference of this kind can be made. They studied the thermal isomerization of a photochromic probe in a group of polymer films, and from the bleaching kinetics of the probe they were able to derive free volume distributions in the host matrices.

We have now found that the distribution of site reactivities may be inferred from the change of quantum yield during irradiation of a photoreactive solid. It is generally observed[18-20] that in amorphous solids the quantum yield of a photoreaction decreases as irradiation progresses. Figure 1 shows a typical example. It refers to a film of poly(vinyl cinnamate), a photopolymer in which cycloaddition between adjacent cinnamoyl groups[21] occurs on irradiation. In the figure, the quantum yield of the reaction, ϕ, is plotted as a function of the degree of conversion, x, of the chromophores and can be seen to decrease rapidly with increasing conversion.[22,23] This behavior is attributed to the preferential

* Institute of Imaging Sciences, Polytechnic Institute of Brooklyn, 333 Jay Street, Brooklyn, NY 11201.

(1) Ranby, B.; Rabek, J. F. "Photodegradation, Photooxidation and Photostabilization of Polymers"; Wiley: New York, 1975.
(2) Williams, J. L. R.; Farid, S. Y.; Doty, J. C.; Daly, R. C.; Specht, D. P.; Searle, R.; Borden, D. G.; Chang, H. J.; Martic, P. A. *Pure Appl. Chem.* **1977**, *49*, 523.
(3) Farid, S.; Martic, P. A.; Daly, R. C.; Thomson, D. R.; Specht, D. P.; Hartman, S. E.; Williams, J. L. R. *Pure Appl. Chem.* **1979**, *51*, 241.
(4) Williams, J. L. R.; Daly, R. C. *Prog. Polym. Sci.* **1977**, *5*, 61.
(5) Hirschberg, Y.; Fischer, E. *J. Chem. Soc.* **1952**, 4522; **1954**, 297.
(6) Gegiou, D.; Muszkat, K. A.; Fischer, E. *J. Am. Chem. Soc.* **1968**, *90*, 62.
(7) Garlund, Z. G. *Polym. Lett.* **1968**, *6*, 57.
(8) Priest, W. J.; Sifain, M. M. *J. Polym. Sci.* **1971**, *9A-1*, 3161.
(9) Petrushov, V. I.; Michailik, O. M.; Vorobev, A. A.; Gurman, V. S. *Khim. Vys. Energ.* **1978**, *12*, 53.
(10) Eisenbach, C. D., *Makromol. Chem.* **1978**, *179*, 2489.
(11) Delzenne, G. A. In "Advances in Photochemistry"; Pitts, J., Jr., Hammond, G.; Gollnick, G., Ed.; Vol. II, 1979.
(12) Eisenbach, C. D. *Polymer* **1980**, *21*, 1175.
(13) Eisenbach, C. D. *Makromol. Chem. Rapid Commun.* **1980**, *1*, 287.
(14) Green, G. E.; Stark, B. P. *Chem. Br.* **1981**, *17*, 228.
(15) Smets, G. *J. Polym. Sci., Polym. Chem. Ed.* **1975**, *13*, 2223.
(16) Kryszewski, M.; Nadolski, B. *Pure Appl. Chem.* **1977**, *49*, 511.
(17) Kryszewski, M.; Nadolski, B.; North, A. M.; Pethrick, R. A. *J. Chem. Soc. Faraday Trans. 2* **1980**, *76*, 351.
(18) Reiser, A.; Egerton, P. L. *Photogr. Sci. Eng.* **1979**, *23*, 144.
(19) Cowell, W.; Pitts, J. N. Jr., *J. Am. Chem. Soc.* **1968**, *90*, 1106.
(20) Kryszewski, M.; Lapienis, D.; Nadolski, B. *J. Polym. Sci., Polym. Chem. Ed.* **1973**, *11*, 2423.
(21) Minsk, L. M. U.S. Patent 2 725 372, 1955.

0002-7863/83/1505-5590$01.50/0